BIODIVERSITAS
Volume 25, Number 5, May 2024
Pages: 2170-2182

ISSN: 1412-033X
E-ISSN: 2085-4722
DOI: 10.13057/biodiv/d250535

Identification and pathogenicity of *Ceratocystis manginecans* causing wilt disease on *Acacia mangium* in Sabah, Malaysia

NADZIRAH MOHD YUNUS[1], MANDY MAID[1,♥], WILSON THAU LYM YONG[2], FIONA EVELYN ANTHONY[1,3], MAHMUD SUDIN[1], PAUL W. J. TAYLOR[4]

[1]Forest Plantation and Agroforestry Program, Faculty of Tropical Forestry, Universiti Malaysia Sabah. Jl. UMS, Kota Kinabalu 88400, Sabah, Malaysia. Tel.: +60-883-20000 Ext. 210200, ♥email: mandy21@ums.edu.my
[2]Biotechnology Research Institute, Universiti Malaysia Sabah, Jl. UMS, Kota Kinabalu 88400, Sabah, Malaysia
[3]Research & Development Division, Sabah Forest Development Authority. Kinarut, Kota Kinabalu 88999, Sabah, Malaysia
[4]Faculty of Science, University of Melbourne. Parkville, Victoria 3010, Australia

Manuscript received: 23 January 2024. Revision accepted: 23 May 2024.

Abstract. *Yunus NM, Maid M, Yong WTL, Anthony FE, Sudin M, Taylor PWJ. 2024. Identification and pathogenicity of* Ceratocystis manginecans *causing wilt disease on* Acacia mangium *in Sabah, Malaysia. Biodiversitas 25: 2170-2182.* An alarming incidence of wilt disease has been reported in an *Acacia mangium* plantation in Ulu Kukut, Kota Belud District, Sabah, Malaysia. Infected trees exhibited symptoms such as severe wilting, sapwood discoloration or black lesion, and a fruity-sweet odor emanating from the fermentation exudate at the wound lesion. This is the first investigation of the causal wilt pathogen in a commercial *A. mangium* plantation in Ulu Kukut, located in the western region of Sabah. This study aimed to identify the causal fungal pathogen from infected *A. mangium* trees using morphological characterization and DNA sequence comparisons for the regions of Internal Transcribed Spacer (ITS), beta-tubulin 1 (*bt1*), transcription elongation factor-1 alpha (*tef1*), guanine nucleotide-binding protein subunit beta-like protein (*ms204*), and second largest subunits of RNA polymerase II (*rpb2*). The fungal isolates shared morphological characteristics with the wilt pathogen *Ceratocystis* sp., including a globose base with a long neck-ended tip with ostiolar hyphae. Sequence-based phylogenetic analysis confirmed the identity of *Ceratocystis manginecans*, distinguishing them from all other *Ceratocystis* species. Bioassays inoculating phyllodes and twigs of 1-year-old *A. mangium* trees confirmed that *C. manginecans* was the cause of wilt disease. Confirming the identity of the causal agent of the increasingly destructive and severe wilt disease aids in developing effective disease management strategies for *Acacia*-based plantations.

Keywords: *Acacia mangium*, *Ceratocystis manginecans*, molecular identification, wilt disease

INTRODUCTION

Acacia mangium has emerged as the most common tree species for the plantation sector in tropical and subtropical regions. In Malaysia, it comprised the majority of forest plantations, with a total area of about 816,600 hectares as of 2018. Sarawak state has the largest *A. mangium* plantation at about 403,000 hectares, followed by Sabah with about 300,000 hectares (Lee 2018). It was first introduced to Sabah in 1966 from seeds of a single tree in Mission Beach, Queensland, as a firebreak species to protect pine plantations (Midgley and Turnbull 2003). It grew remarkably well, thus leading to the establishment of the first commercial *A. mangium* plantation in Sabah in 1976 (Udarbe and Hepburn 1986; Unchi 2010). The primary reason for the widespread planting of *A. mangium* is its multipurpose benefits in forestry, agroforestry, and agricultural ecosystems (Epron et al. 2013; Nair et al. 2021). Acacia has the potential to improve poor soil conditions, nutrient cycling, increase carbon sequestration, stimulate microbial and bacterial activity in the soil, serve as an ornamental, and provide wood and charcoal (Bini et al. 2013; Sitters et al. 2013; Lee et al. 2015; Koutika and Richardson 2019). With the expansion of commercial *A. mangium* plantations, the species became vulnerable to various diseases, such as heart rot (Mohammed et al. 2006; Jha 2020; Farid et al. 2023), pink disease (Ambrose et al. 2022), Ganoderma root rot (Glen et al. 2009; Coetzee et al. 2011; Gill et al. 2018; Suryantini and Wulandari 2018)), phyllode rust and stem canker (Suryantini and Wulandari 2018; Lelana et al. 2020; Maid et al. 2018). Adding to the challenges, Lee (2018) reported wilt disease caused by the *Ceratocystis* pathogen, introducing a new dimension to the plantation's health considerations. Despite this, effective management strategies for this pathogen are still viable.

The first instance of wilt disease caused by the *Ceratocystis*, was discovered in a plantation of *A. mangium* in Peninsular Malaysia in 2009. Symptoms included the appearance of a black lesion or sapwood discoloration followed by the formation of canker and sunken or cracked areas above the canker area on the stems and branches. As the infection progresses, the phyllodes turn yellow, and the tree rapidly wilts due to water deficiency (Tarigan et al. 2011a; Brawner et al. 2015), which results in the death of trees and the dieback symptom. Root rot is another symptom of *C. manginecans* infections (Oliveira et al. 2015). An outbreak can spread over short distances via root anastomosis, contaminated pruning equipment (Lehtijärvi et al. 2018), or wood dust (EFSA Panel on Plant Health et al. 2016). In addition, the wounds on the stem produce

exudate, foam, and later gummosis, which attracts ambrosia and nitidulid beetles and likely spreads the disease (Al Adawi et al. 2013; Brawner et al. 2015; Wingfield et al. 2017).

The vulnerability to infection is heightened by various factors, including exposed wounds caused by mammals and wood-boring insects such as elephants, wild hogs, monkeys, and ambrosia beetles. Furthermore, human activities, such as pruning and singling in silvicultural programs have been identified as contributors to increased infection risks (Tarigan et al. 2011b; Syazwan et al. 2021). The invasion of fungi through these wounds plays a critical role in compromising the integrity of xylem vessels, consequently disrupting the host metabolism (Yadeta and Thomma 2013; Kashyap et al. 2021). The prevalence of vascular wilt disease symptoms ranged from 50-60% in Sipitang and Pitas, Sabah. Young *A. mangium* stands injured by silvicultural management, such as pruning were more susceptible to wilt disease (Maid and Ratnam 2014). Then, a preliminary survey was conducted in 2020 at Sabah Forest Development Authority (SAFODA) *Acacia* plantations, Ulu Kukut, the severity of *Ceratocystis* infections was alarming, affecting more than 50% of the trees (F. E. Anthony, personal communication). Most of the wilt-infected trees decline and result in death. The rapid spread of *Ceratocystis* has compelled the acacia industries to switch to alternative tree species, such as *Eucalyptus pellita*, to avoid substantial losses (Lee 2018) and break the disease cycle.

Even though, the signs and symptoms of wilt were observed on *A. mangium* plantations in the eastern region of Sabah and on ten *A. mangium* trees in Sarawak in late 2011, but the identity of the fungus was not confirmed (Lee 2018). Other countries in Southeast Asia have also suffered significant losses because of infection by *C. manginecans* and *C. acaciivora*, as reported in Indonesia (Tarigan et al. 2011a), Vietnam (Thu et al. 2012; Trang et al. 2018), and Thailand (Pornsuriya and Sunpapao 2015). Despite the identification of *C. acaciivora* as the wilt pathogen of *A. mangium* in Tawau, Sabah (Brawner et al. 2015), and other locations in Malaysia such as Johor, Pahang, and Sarawak where *C. fimbriata* was also noted (Syazwan et al. 2021), accurate molecular confirmation was lacking, and identification was primarily based on morphological analyses. Notably, Barnes et al. (2023) recently confirmed that *C. manginecans*, rather than *C. fimbriata*, is the causative fungal agent of wilt in infected *A. mangium* in Malaysia. Interestingly, *A. auriculiformis* and *A. crassicarpa* demonstrated greater tolerance to *C. manginecans* infections than *A.* mangium (Barnes et al. 2023). Additionally, Lapammu et al. (2023) reported that among 180 *A. mangium* clones, 50 exhibited tolerances to *C. manginecans*, presenting potential applications in establishing seed orchards and breeding programs alongside other tolerant *Acacia* species (Wingfield et al. 2023).

The purpose of identifying the causal agent of the wilt disease is to link the knowledge of their biology and potential risk so that SAFODA can develop appropriate integrated management strategies in the *Acacia* plantations. The objectives of this study were to (i) isolate and identify of *Ceratocystis* species using fungal morphological characteristics and molecular markers, and (ii) to confirm the pathogenicity by laboratory and greenhouse inoculations on 1-year-old *A. mangium trees*.

MATERIALS AND METHODS

Fungal isolation

A disease survey was conducted in August 2020 on an 88 hectares *A. mangium* plantation planted in 2011 by SAFODA in Ulu Kukut (6°31’37” N, 116°35’46” E). The trees were examined from ground level to 1.5 m height for stem and branch symptoms associated with wilt disease. Woods, phyllodes, roots, and soil samples were collected from five symptomatic *A. mangium* stands in the plantation and wrapped in paper towels to keep them moist before being delivered to the pathology laboratory at the University Malaysia Sabah (UMS). Sapwoods with internal discoloration were cut into pieces (10x10 mm) and sterilized by soaking in 2.5% a.i. sodium hypochlorite (diluted from commercial Clorox), followed by 75% ethanol, and then washed with distilled water thrice. All samples were placed in a Petri dish containing 2% Malt Extract Agar (MEA) (Millipore, Germany) and 25 mg/L penicillin and incubated at 25°C for 14 days. The diameter of colonies was measured daily for up to 14 days. The data was statistically analyzed using one-way Analysis of Variance (ANOVA) in IBM SPSS Statistics for Windows, Version 28.0 (IBM Corp. 2021).

Culture characteristics and morphology

The morphology of isolated fungi was studied using macroscopic and microscopic observations. Macroscopic features, included texture, shape, odor, and color both front and reverse view of the isolates. Microscopic features, such as hyphae, septa, ascomata, ascospores, phialides and conidial forms were observed using the cellSens Dimension 1.9 imaging software on an Olympus BX53 light microscope (Evident Corporation, Tokyo, Japan).

DNA extraction

Mycelia (150 mg) of 7-day-old cultures of *Ceratocystis* isolates were transferred to 1.5 mL Eppendorf tubes using a sterile scalpel. The tubes were then filled with 500 µL of extraction buffer (10 mL CTAB, 0.3 g Polyvinyl pyrrolidone, 20 µL B-Mercaptoethanol) and placed in a thermomixer (Eppendorf thermomixer comfort, Hamburg, Germany) for 30 min at 300 rpm at 60°C. Then, phenol:chloroform:isoamyl alcohol (25:24:1) was added to the tubes and inverted for 2 min before centrifuging (Eppendorf 5417R, Germany) for 10 min at 13,000 rpm at 4°C. The visible aqueous phase was transferred to new tubes, and an equal volume of chloroform: isoamyl alcohol (24:1) was added and inverted for 2 min before centrifuging at the same setting. The upper layer of the supernatant was collected in separate tubes, and an equal amount of isopropanol was mixed and inverted for 5 min before being left at 20°C for 2-3 h. The samples were centrifuged for 10 min at 13,000 rpm at 4°C. After

removing the supernatant, the pellets were washed twice with 500 µL of 70% ethanol before centrifuging. The ethanol was removed, and pellets were air-dried in a vacuum centrifugal concentrator (Concentrator plus, Germany) for 10 min at 45°C. After that, DNA pellets were dissolved in 50 µL of TE buffer and stored at -20°C. The concentration of DNA was measured using a Nanodrop spectrophotometer (Nanodrop 2000, Thermo Fisher Scientific, USA).

Polymerase Chain Reaction (PCR) amplification

The fungal isolates were subjected to phylogenetic analysis using partial regions of the following loci: Internal transcribed spacer and the intervening 5.8S region (ITS) of the rDNA using primers ITS1 and ITS4, beta-tubulin 1 (*bt1*) gene using primers Bt1a and Bt1b, transcription elongation factor-1 alpha (*tef1*) gene using primers EF1F and EF2R, guanine nucleotide-binding protein subunit beta-like protein (*ms204*) gene using primers MS204F.ceratoB and MS204R.ceratoB, and second largest subunits of RNA polymerase II (*rpb2*) gene using primers RPB2-5Fb and RPB2-7Rb (Table 1). The PCR amplification programs for all primers included steps of initial denaturation, followed by 39 cycles of denaturation and annealing, and final extension using the Thermal cycler (PTC-200, MJ Research, Basel, Switzerland) under the conditions detailed in Table 1. The PCR reaction mixtures of 25 µL contained 1 µL of each primer (10 mM), 2 µL of 10 mM dNTP mix, 2.5 µL of PCR 10× concentration buffer, 5 µL of DNA template, 0.5 µL of *Taq* DNA polymerase, and 12.5 µL of sterile distilled water. The successful PCR amplicons were identified by electrophoresis (Mupid-exU ADVANCE, San Francisco, CA) on 2% agarose gels, stained with ethidium bromide and visualized under UV illumination (BioRad Gel Doc™ XR$^+$, USA).

Sequencing and phylogenetic analysis

The PCR amplicons were sent to Apical Scientific Sdn. Bhd. For sequencing in both directions. The raw sequence data were edited with Bioedit software (https://bioedit.software.informer.com/7.2/) to combine the forward and reverse sequences into consensus sequences. The consensus sequences were then subjected to an initial BLAST search against the National Center for Biotechnology Information (NCBI) GenBank database (http://www.ncbi.nlm.nih.gov) to identify the *Ceratocystis* species and biogeographic clade of the isolates from SAFODA, Ulu Kukut. The consensus sequence reads and published sequences were aligned in MEGA11 software (https://www.megasoftware.net/) using the MUSCLE program for phylogenetic tree construction (Tamura et al. 2021). Maximum Likelihood (ML) analysis was used to construct phylogenetic trees on individual gene datasets and a combined dataset of five genes (Newman et al. 2016). Before constructing the phylogenetic tree, each dataset was run through MEGA11 software to determine the best model for each dataset. The confidence values of the nodes were calculated using 1000 bootstrap repetitions. A Partition Homogeneity Test (PHT) implemented in PAUP was used to determine whether there was a conflict between the datasets before performing a combined analysis for the sequences of the five gene loci. In addition to the ML, the phylogenetic tree was constructed using Bayesian analysis in MrBayes version 3.2.7 (https://nbisweden.github.io/MrBayes/) with 1 million generations and the Markov Chain Monte-Carlo algorithm (MCMC) with four chains, with samples taken for every 1000th tree. The generated tree was edited using Fig Tree (http://tree.bio.ed.ac.uk/software/figtree/). In both ML and Bayesian analysis, *Huntiella chlamydoformis* was used as the outgroup taxon for both the individual gene datasets and the combined gene datasets.

Table 1. List of primers and PCR conditions

Regions	Primer Sequence (5'-3')	PCR Conditions	References
ITS	ITS1: TCC GTA GGT GAA CCT GCG GITS4: TCC TCC GCT TAT TGA TAT GC	Denaturation: 96°C, 2 min; 39 cycles: 94°C, 20 sec; 55°C, 40 sec; Extension: 72°C, 10 min.	Glass and Donaldson (1995) Al-Bedak et al. (2018)
bt1	Bt1a: TTC CCC CGT CTC CAC TTC TTC ATGBt1b: GAC GAG ATC GTT CAT GTT GAA CTC	Denaturation: 96°C, 2 min; 39 cycles: 94°C, 20 sec; 55°C, 40 sec; Extension: 72°C, 10 min.	Glass and Donaldson (1995) Lopes et al. (2014)
tef1	EF1F: TGC GGT GGT ATC GAC AAG CGT EF2R: AGC ATG TTG TCG CCG TTG AAG	Denaturation: 96°C, 2 min; 39 cycles: 94°C, 20 sec; 55°C, 40 sec; Extension: 72°C, 10 min.	Jacobs et al. (2004), Lopes et al. (2014)
ms204	MS204F.ceratoB: GGC TGA GCA GCT GAT CCT T MS204R.ceratoB: ATG TCC GGG TAG TGT TAC CG	Denaturation: 96°C, 10 min; 39 cycles: 94°C, 30 sec; 55°C, 54 sec; 72°C, 1 min; Extension: 72°C, 10 min.	Fourie et al. (2015)
rpb2	RPB2-5Fb: GAY GAY CGT GAT CAC TTY GG RPB2-7Rb: CCC ATR GCY TGY TTR CCC AT	Denaturation: 96°C, 10 min; 39 cycles: 94°C, 30 sec; 55°C, 54 sec; 72°C, 1 min; Extension: 72°C, 10 min.	Fourie et al. (2015)

Pathogenicity test

Laboratory test

The pathogenicity of isolated *Ceratocystis* species was determined by inoculation on phyllodes and twigs of 1-year-old *A. mangium*. Each isolate was tested with ten phyllodes and ten twigs, each with three replicates, while another set of ten phyllodes and ten twigs served as a control. All excised tissues were washed sequentially with 2.5% a.i. sodium hypochlorite, followed by 75% ethanol, and distilled water. Wounds were made with a sterile scalpel on the surface of twigs and phyllodes. The isolates were cut from the edges of actively growing colonies with a sterile cork borer (5 mm diameter) and then inoculated, facing downward on the surface of the wounds, while 2% sterile MEA plugs were used for control treatment as described by Tarigan et al. (2011a). The inoculated phyllodes and twigs were sealed in individual bags with sterilized moist tissue paper inside to maintain humidity (70-80%) and kept at room temperature (26-28°C). The lesions were observed daily for five days, and their length and width (mm) were measured with a caliper. Fungi re-isolated from the inoculated phyllodes and twigs and their morphological characteristics were compared to the original fungi used for inoculation and isolated from infected sapwoods. The lesion length was analyzed using descriptive analysis, ANOVA with Tukey post-hoc test, and ranking of lesion length based on the fungal isolate.

Greenhouse test

A total of 75 seedlings of 1-year-old *A. mangium* were used for the pathogenicity trial, with five seedlings for each of the three replicates for each isolate and control. The greenhouse temperature was maintained at 28±2°C for optimum seedling growth, and the seedlings were watered twice daily. The raised seedlings were thoroughly inspected before inoculation to ensure they were disease-free and undamaged, particularly on the phyllodes and stems. After spraying the stem with 75% ethanol and wounding with a sterile scalpel approximately 14 cm from the bottom of the stem, a 5 mm diameter 2% MEA plug with respective isolate (12-day-old) was carefully placed with an inoculating needle facing down onto the wound surface and immediately sealed with parafilm to prevent contamination. The control was 2% MEA sterile plug. The resulting lesions were measured ten days after inoculation, and disease symptoms in the seedlings were observed. The pathogen responsible for the disease was re-isolated using three different methods tailored to efficiency: (1) by extracting a small portion of the lesion and transferring it to 2% MEA (Millipore, Germany) supplemented with 25 mg/L Penicillin, (2) by sandwiching the lesion stem between circular carrot slices (approximately 4 cm in diameter), sealing it with Parafilm (Bemis Company, Inc.) for 3-5 days until the carrot developed a fruiting body, which was then transferred to MEA (Moller and DeVay 1968; Tarigan et al. 2011a; Syazwan et al. 2021), and (3) by directly transferring the spores from the sporulating stems to MEA plates using a sterile needle. The re-isolated isolates obtained through any of the aforementioned methods were reassessed based on their morphology, and the results were compared to the original samples obtained through fungal isolation from infected sapwoods for validation. The lesion length was analyzed using descriptive analysis, ANOVA with Tukey post-hoc test, and ranking of lesion length based on the fungal isolate.

RESULTS AND DISCUSSION

Characteristics and morphology of fungal isolates

Symptoms of wilt disease during the survey included the appearance of black lesions or discoloration of the sapwood, followed by canker formation and sunken or broken areas on stems and branches above the canker area. As the infection progressed, the phyllodes turned yellow and the trees rapidly wither due to lack of water. Fruiting bodies of fungi were also seen on the stem of *A. mangium* (Figure 1). Out of all the samples collected during the disease survey, including wood, phyllodes, roots, and soil, *Ceratocystis* isolates were exclusively detected in the wood samples. Four distinct *Ceratocystis* isolates were identified using morphological characteristics, such as surface topography, texture, pigmentation, and mycelium. The four isolates displayed a diverse range of macroscopic features (Figure 2), including varying average diameter growth within 14 days (Figure 3). Although all isolates demonstrated optimal growth at 25°C, isolates 4 and 5 displayed nearly identical growth rates over the 14 days, reaching 8 and 7.9 cm, respectively. Isolate 1 exhibited the slowest growth among the four isolates, measuring 5.1 cm in diameter, while isolate 6 measured 6 cm in diameter.

The macroscopic features in Figure 2 show that isolate 1 had a matted pale olivaceous grey colony and a dark brown to black reverse side; isolate 4 had a circular greyish colony that turned darker grey with age, and the reverse side was circular brown to black; and isolate 5 had white-color colony that turned greyish brown with age, and the reverse side was dark brown to black. Isolate 6 developed a dark grey olivaceous colony with a brownish-to-black reverse side. All isolates produced a sweet, fruity banana-like aroma and dark brown to black long-neck perithecia, typical of *Ceratocystis* species. An abundance of sticky masses adhered to the apex of the perithecia, which changed color from cream to orange as they aged and contained various substances such as mucilage or other secretions produced by the fungus. In addition, the isolates had globose or obpyriform ascomata bases and a long neck-ended tip with diverging ostiolar hyphae. They also had hat-shaped hyaline ascospores and two different types of hyaline conidia: cylindrical and barrel-shaped. Aleuroconidia had thick walls, an ovoid shape, and a smooth surface, grouped singly or in basipetal chains. Figures 4 to 7 show the morphological characteristics of *Ceratocystis* isolates 1, 4, 5, and 6.

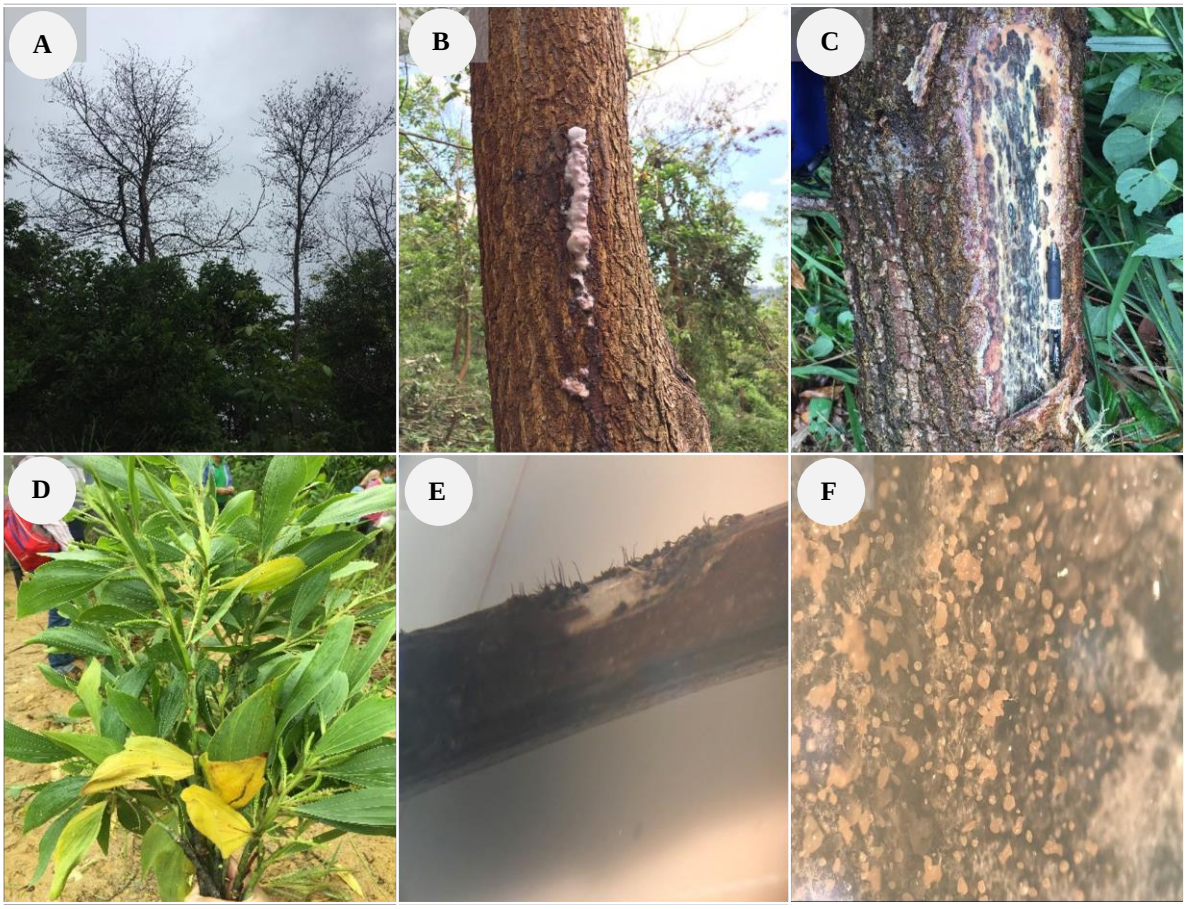

Figure 1. Typical symptoms associated with *Ceratocystis* disease: A. severe wilting and death of infected *Acacia mangium* trees; B. Presence of fruity-smelling foam at the wound lesion; C. Infected sapwood with blue-black lesion; D. Yellowing of the young leaves; E. Fruiting bodies of *C. manginecans* on *A. mangium* stem; F. Sticky masses adhering to the apex of the perithecia

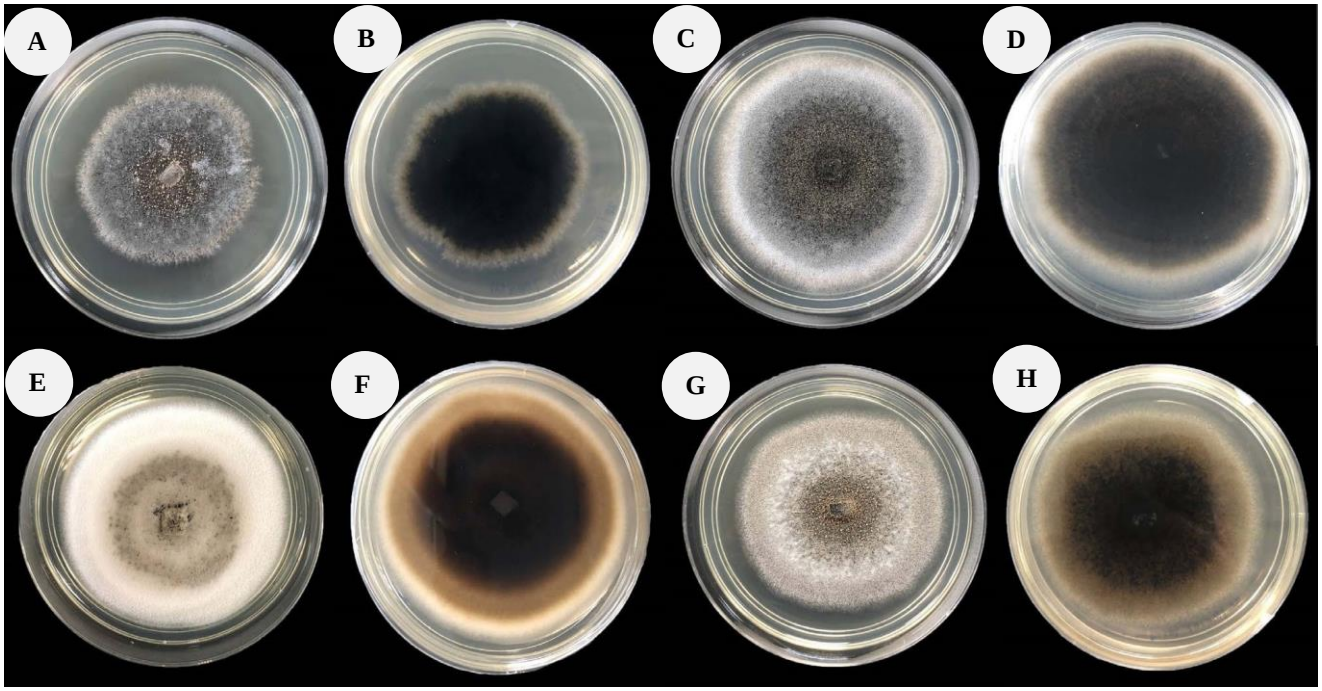

Figure 2. Macroscopic features of *Ceratocystis* isolates: A. Front and B. Reverse view of isolate 1; C. Front and D. Reverse view of isolate 4; E. Front and F. Reverse view of isolate 5; and G. Front and H. Reverse view of isolate 6

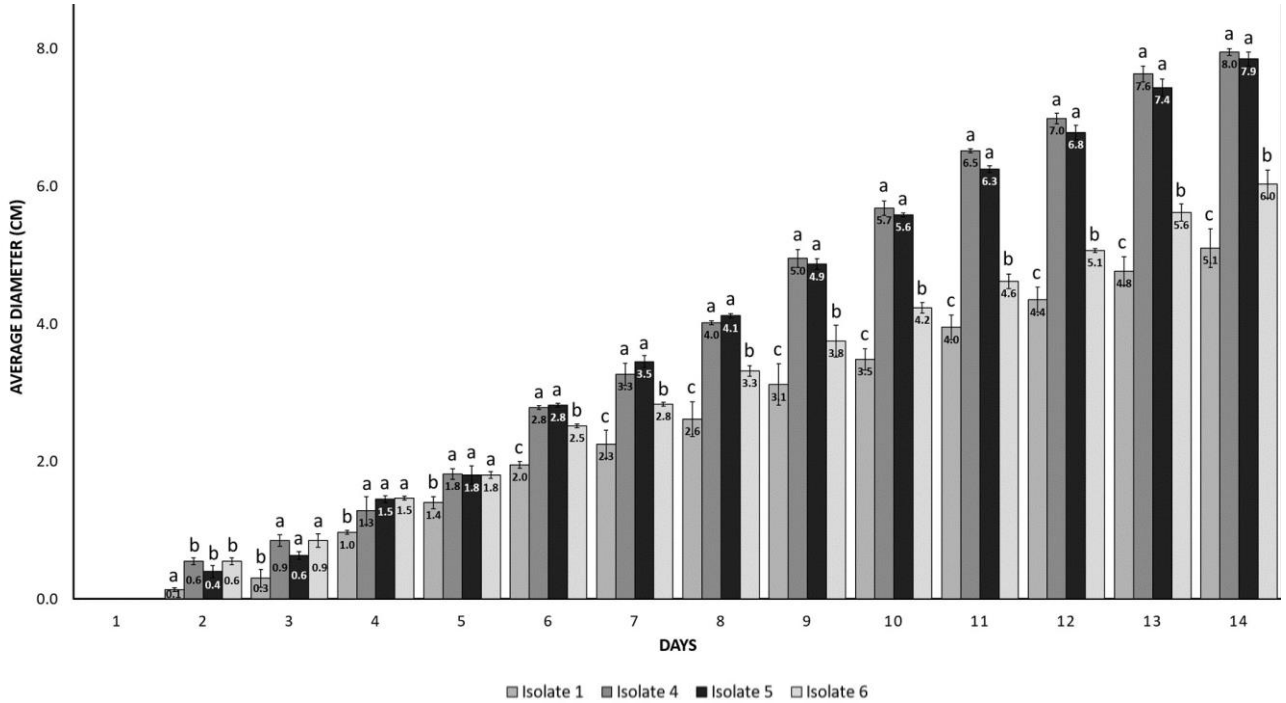

Figure 3. The average diameter (cm) growth of *Ceratocystis* isolates in 14 days. Different letters indicate significant differences between groups (p<0.05). Values represent means ± SE (n = 3)

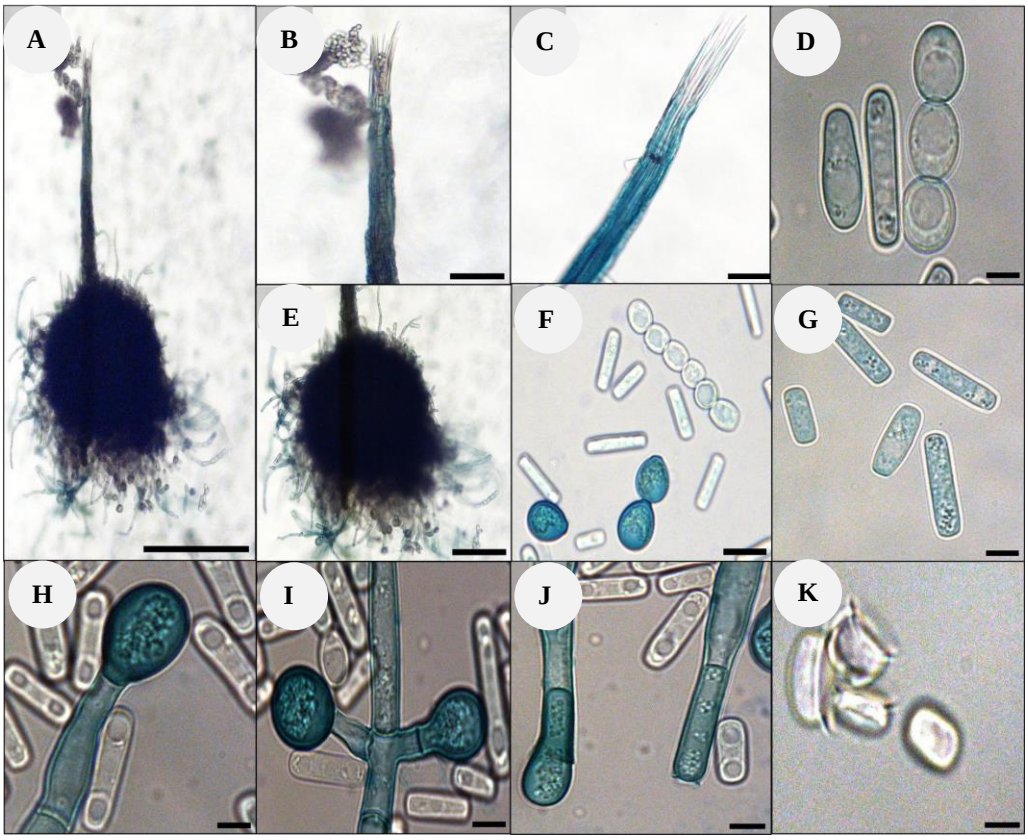

Figure 4. Morphological characteristics of *Ceratocystis* isolate 1: A. The full structure of perithecium; B. Divergent ostiolar hyphae; C. Straight ostiolar hyphae; D. Cylindrical conidia and rounded conidia in a chain; E. Globose base; F. Aleurioconidium, conidia in chain, and cylindrical conidia; G. Cylindrical conidia; H, I. Terminal thick-walled aleurioconidium; J. Flask-shaped phialide (conidiophores) producing cylindrical conidia; and K. Top and side views of hat-shaped ascospores. Scale bars: (A) = 200 μm; (B, E) = 50 μm; (C, F) = 20 μm; and (D, G, H, I, J, K) = 5 μm

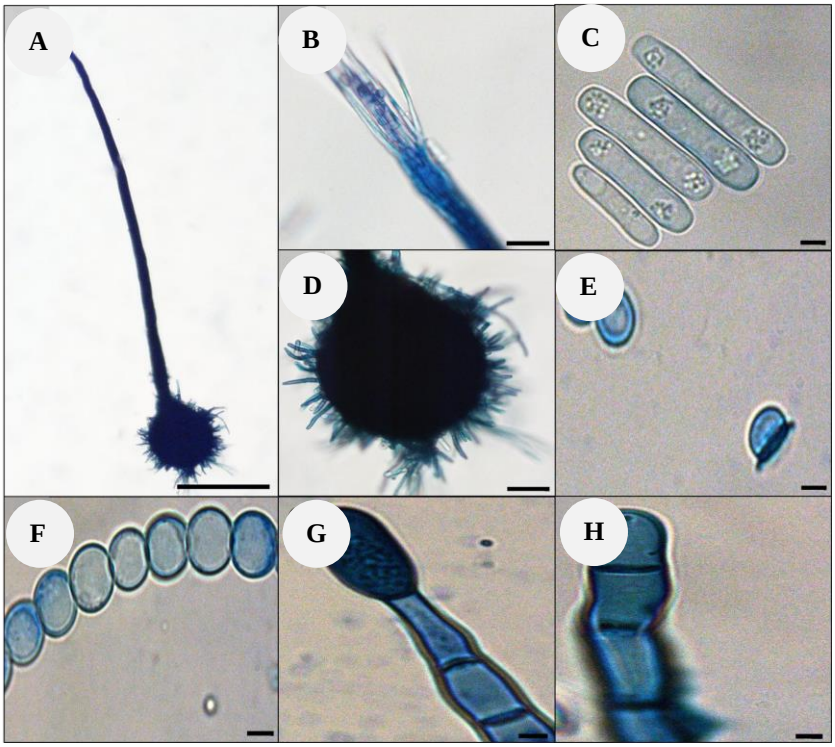

Figure 5. Morphological characteristics of *Ceratocystis* isolate 4: A. The full structure of perithecium; B. Divergent ostiolar hyphae; C. Cylindrical conidia; D. Obpyriform base; E. Top and side views of hat-shaped ascospores; F. Round-shaped conidia in chain; G. Terminal thick-walled aleurioconidium; and H. Typical submerged septate hyphae. Scale bars: A. = 200 µm; (B, D) = 20 µm; (C, E, F, G, H) = 5 µm

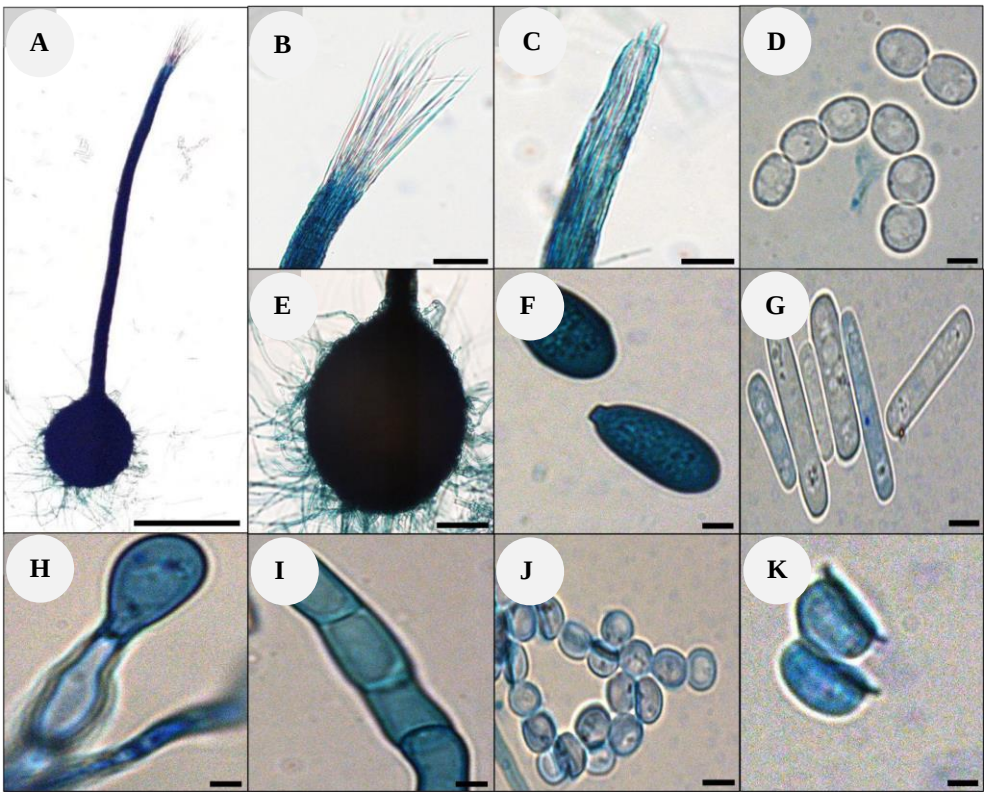

Figure 6. Morphological characteristics of *Ceratocystis* isolate 5: A. The full structure of perithecium; B. Divergent ostiolar hyphae; C. 247 straight ostiolar hyphae; D. Round-shaped conidia in chain; E. Globose base; F. Aleurioconidium; G. Cylindrical conidia; H. Terminal 248 thick-walled aleurioconidium; I. Typical submerged septate hyphae; and (J, K) top and side views of hat-shaped ascospores. Scale bars: (A) = 200 µm; (B, C, E) = 20 µm; (D, F, G, H, I, J, K) = 5 µm

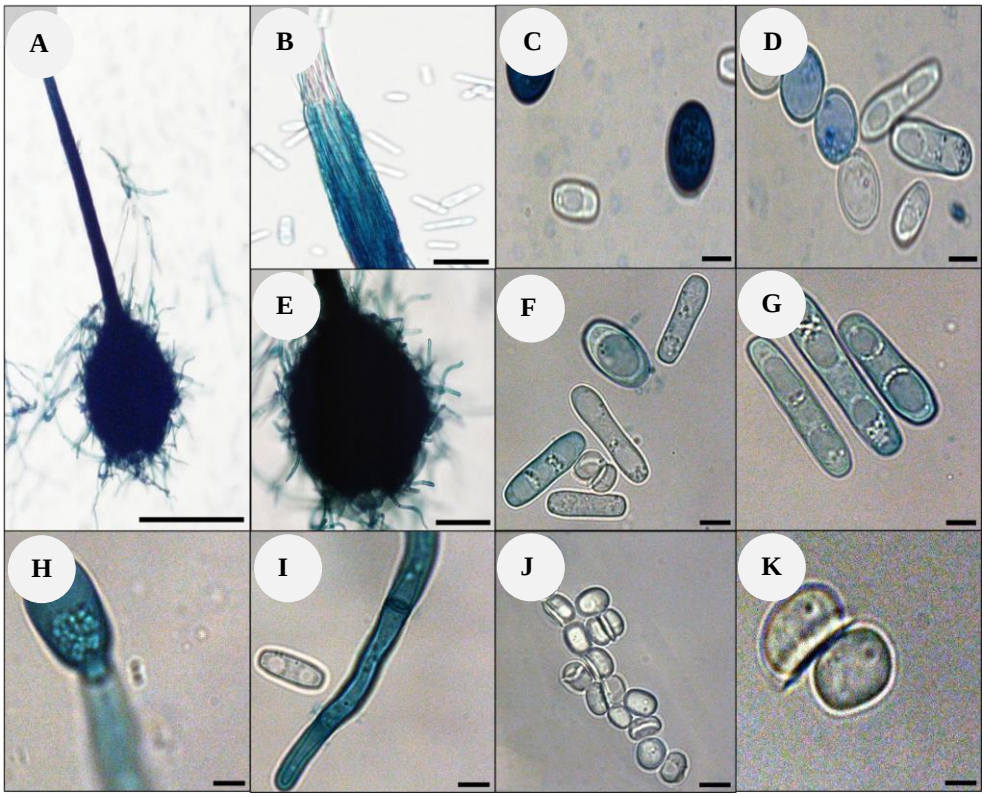

Figure 7. Morphological characteristics of *Ceratocystis* isolate 6: A. The full structure of perithecium; B. Short divergent ostiolar hyphae; C. Aleurioconidium; D. Round-shape conidia in chain and cylindrical conidia; E. Obpyriform base; F. Barrel-shaped conidia and cylindrical conidia; G. Cylindrical conidia; H. Terminal thick-walled aleurioconidium; I. Typical submerged septate hyphae; and (J, K) top and side views of hat-shaped ascospores. Scale bars: (A) = 200 µm; (B, E) = 20 µm; (C, D, F, G, H, I, J, K) = 5 µm

PCR amplification, sequencing and phylogenetic analysis

The nucleotide sequences of PCR-amplified ITS (~600 bp), β-tubulin (~600 bp), TEF (~700 bp), MS204 (~800 bp), and RPB2 (1000 bp) regions from *Ceratocystis* isolates were deposited in GenBank (Table 2). Based on initial BLAST searches in GenBank, the sequences revealed that isolates from SAFODA, Ulu Kukut, Sabah, were 100% similar to *C. manginecans*, *C. fimbriata*, and *C. acaciivora*, posing challenges in resolving the species identification using any singlegene locus. The Maximum-likelihood tree clustering method was used to construct phylogenetic trees for the fungal isolates based on the ITS, β-tubulin, TEF, MS204 and RPB2 genes regions. The final dataset included the following nucleotides and characters: ITS (34 nucleotides, 582 characters), β-tubulin (34 nucleotides, 507 characters), TEF (34 nucleotides, 779 characters), MS204 (33 nucleotides, 857 characters) and RPB2 (33 nucleotides, 1079 characters).

Among the five constructed single-gene trees, the ITS tree provided the best resolution for separating the isolates from the aligned sequences. In contrast, the β-tubulin, TEF, MS204, and RPB2 single-gene trees could not differentiate between some closely related species. Specifically, the β-tubulin gene tree was unable to differentiate between the species *Ceratocystis manginecans*, *C. eucalypticola*, *C. curvata*, *C. acaciivora* and *C. polyconidia*; the TEF gene tree was unable to differentiate between *C. manginecans*, *C. eucalypticola*, *C. fimbriata*, *C. acaciivora*, and *C. fimbriatomima*; the MS204 gene tree was unable to differentiate between *C. manginecans*, and *C. acaciivora*; and the RPB2 gene tree was unable to differentiate between *C. eucalypticola*, *C. acaciivora*, *C. manginecans*, and *C. polyconidia.*

Phylogenetic analysis using the combination of five gene regions allowed the four *Ceratocystis* isolates to be identified as *C. manginecans* (Figure 8). Using 1000 replicates, partition homogeneity tests (PHT) for the five gene regions yielded a *p*-value of >0.05 (= 1.00), showing that the datasets for the five loci are not identical. The analysis of the concatenated multiple genes involved 34 nucleotide sequences, mostly from ex-type strains, with the final datasets containing 3872 characters. Both the MP and Bayesian analyses of the datasets generated trees with generally consistent topologies and evolutionary relationships between taxa.

Table 2. List of *Ceratocystis* isolates and GenBank accession numbers for analyzed sequences

Isolates	Species	GenBank accession no.				
		ITS [a]	β-tubulin [b]	TEF [c]	MS204 [d]	RPBII [e]
1	*Ceratocystis manginecans*	OP964449	OQ507133	OQ550946	OQ550950	OQ550954
4	*Ceratocystis manginecans*	OP964450	OQ507134	OQ550947	OQ550951	OQ550955
5	*Ceratocystis manginecans*	OP964451	OQ507135	OQ550948	OQ550952	OQ550956
6	*Ceratocystis manginecans*	OP964452	OQ507136	OQ550949	OQ550953	OQ550957

Note: [a] ITS: Internal transcribed spacer, [b] β-tubulin: beta-tubulin 1, [c] TEF: transcription elongation factor-1 alpha [d] MS204: guanine nucleotide binding protein subunit beta-like protein [e] RPBII: second largest subunits of RNA polymerase II

Figure 8. Molecular phylogenetic tree constructed using maximum likelihood (ML) analysis of concatenated multiple gene loci (ITS, *bt1*, *tef1*, *ms204*, and *rpb2*). Each node represents the bootstrap values of ML and Bayesian posterior probabilities. The ex-type strain of each species is indicated by [T]. Isolates highlighted in square box are from SAFODA, Ulu Kukut, and two closely related *C. manginecans* species

Figure 9. Pathogenicity in Greenhouse: A. Lesion on stem isolate 1; B. Lesion on stem isolate 4; C. lesion on stem isolate 5; D. lesion on stem isolate 6

Pathogenicity test

Healthy detached phyllodes and twigs from *A. mangium* seedlings exhibited varying-sized lesions within two days of laboratory inoculation, confirming the pathogenicity of all isolated fungi. Lesions on the phyllodes ranged from 6.4 to 23.8 mm, while those on the twigs varied between 12.3 and 16.3 mm. Notably, isolate 4 produced the longest lesions on phyllodes, measuring 23.8 mm, while isolate 5 induced the longest lesion on twigs, measuring 16.3 mm. Re-isolation of the pathogen from lesions on inoculated phyllodes and twigs consistently yielded morphologically identical *Ceratocystis* isolates.

In the greenhouse inoculation trials, all four isolates of *C. manginecans* species exhibited a pronounced pathogenicity towards *A. mangium* seedlings (Figure 9). After ten days of inoculation, symptoms comparable to those observed during the laboratory pathogenicity test appeared. Over time, additional symptoms emerged, including wilting, defoliation, and pale green and yellow foliage manifestations, resulting in seedling death. In contrast, the seedlings in the control group remained healthy and symptomless. Lesions on diseased *A. mangium* stems varied in length from 159.0 to 516.0 mm, with isolate 1 causing the longest lesion (516.0 mm) and isolate 4 the shortest (243.0 mm). Koch's postulates were confirmed through re-isolations, demonstrating that the obtained isolates were indeed responsible for the disease symptoms in the *A. mangium* host. A morphological examination further revealed that the laboratory and greenhouse's re-isolated isolates exhibited identical characteristics to the original samples obtained through fungal isolations from infected sapwoods. The most effective method for re-isolating *Ceratocystis* was by sandwiching the lesioned stem between carrot slices and directly transferring the spores to MEA (Millipore, Germany) plates from sporulating stems using a sterile needle. In the control phyllodes and twigs, no symptoms were observed.

Discussion

The pathogen responsible for the extensive wilting of *A. mangium* observed in plantation in SAFODA, Ulu Kukut, Sabah, is *C. manginecans*, a fungal species that causes various disease symptoms such as vascular discoloration and partial or complete wilt of affected trees that develop after pruning activities. Species identification was based on morphological characteristics and DNA sequence data comparison. The use of phylogenetic analysis is imperative to accurate species identification, as it provides a comprehensive understanding of evolutionary relationships and aids in distinguishing closely related species with similar morphologies (Naranjo-Ortiz and Gabaldón 2019; Li et al. 2021).

Four morphologically distinct isolates were identified from symptomatic *A. mangium* trees, and all isolates were identified as *C. manginecans* to its closest evolutionary neighbour based on sequencing data comparisons using single gene and concatenated multiple gene phylogenetic analysis. Although the morphological identification shows differences between those four isolates, they all belong to the same species because they were clade closely in all phylogenies, indicating that they are genetically similar to each other, and their clade is closely related to *C. manginecans* isolated from mango wilt disease in Oman and Pakistan (Al Adawi et al. 2013, 2014). *Ceratocystis manginecans* has decimated numerous trees in those countries, spreading to 12 districts in Oman and three in Pakistan, and has had a detrimental impact on mango cultivation, causing significant losses and posing challenges for farmers and overall mango production in the affected regions (Van Wyk et al. 2007; Al Adawi et al. 2013, 2014). This study also confirmed that the isolates responsible for severe wilt in Ulu Kukut are the same species that killed *A. mangium* in Indonesia (Tarigan et al. 2011a) and Vietnam (Fourie et al. 2016). The *C. manginecans* populations from Malaysia are not clonal, and Southeast Asia is the centre of its genetic diversity (Fourie et al. 2016).

The concatenated phylogenetic analysis provides clear evidence that *C. manginecans* found in *A. mangium* from Ulu Kukut can be easily distinguished from the *C. acaciivora* and *C. fimbriata* species complex based on comparisons of DNA sequences. Although *C. fimbriata* and *C. manginecans* were once considered a single taxon, recent research, such as that conducted by Fourie et al. (2015), has demonstrated that *C. manginecans* should be recognized as a distinct species to *C. fimbriata* that affects sweet potatoes. *Ceratocystis fimbriata* isolated from sweet potato in Sabah did not infect the three *Acacia* spp. in a pathogenicity test (Barnes et al. 2023). Furthermore, Tarigan et al. (2011a) found that *C. manginecans* was most closely related to *C. acaciivora*, the pathogen responsible for a destructive canker and wilt disease affecting *A. mangium* plantations in Indonesia. However, subsequent DNA analysis concluded that *C. manginecans* and *C. acaciivora* should be considered synonymous and referred to as *C. manginecans* (Fourie et al. 2015). These two species are rarely differentiated in β-tubulin, TEF, MS204, and RPB2 phylogenetic analyses, raising significant doubts over the authenticity of the *C. acaciivora* species.

The pathogenicity of *C. manginecans* isolates to *A. mangium* was confirmed through inoculation trials in the laboratory and greenhouse. Following the inoculation, all four isolates developed lesions on the detached phyllodes and twigs and the stems of 1-year-old seedlings. Although the seedlings were alive after ten days of inoculation, they displayed wilting symptoms due to the infection, which would inevitably lead to mortality if the infection progressed further. Based on survey in the present study in the Ulu Kukut *Acacia* plantation, certain silvicultural practices, such as pruning, can potentially increase the susceptibility of trees to infection by creating entry points for the pathogen. The presence of stem wounds, particularly those caused by pruning activities, plays a significant role in disseminating *Ceratocystis* infections. Pruning is an essential silvicultural practice commonly used in many *A. mangium* plantations to improve the straightness of the stands (Hegde et al. 2013). It directly impacts the overall health, stability, and visual appearance of the trees. Although pruning is a necessary practice, especially for trees with multiple leaders that lack self-pruning ability like *A. mangium*, it is important to recognize that the infections could have originated from improper pruning techniques such as contaminated pruning saw (Farid et al. 2018) or even through the workers' clothing and shoes, which could have carried the pathogen (Raupp and Gonthier 2017; Friday et al. 2015). According to Maid and Ratnam (2014), the incidences of wilt diseases were considerably higher in pruning sites within *A. mangium* plantations.

Improper pruning techniques, such as using contaminated equipment, wood dust from infected stands, and root anastomosis, all played a significant role in the spread of the disease during the outbreak. According to Chi (2022), a pathogenicity trial of *C. manginecans* on *Acacia* roots revealed that the roots were vulnerable to *C. manginecans*, implying that root damage should be minimized in the planting stock and after out-planting in the field to minimize losses. Rapid removal of infected trees and other control measures such as thorough cleaning and sterilization of pruning equipment to limit short-distance dissemination could be an effective strategy in limiting disease spread (Chi et al. 2019). More importantly, proper wound management and avoiding unnecessary stem injuries can help to reduce the spread of *Ceratocystis* infections and their impact on susceptible plant species. Despite a positive correlation between vascular wilt disease incidence and pruning activity, Maid and Ratnam (2014) reported that the correlation is considerably lower in properly pruned *Acacia* stands.

In conclusion, in the present study *C. manginecans* was identified as the causative agent of wilt diseases isolated from harvested symptomatic sapwood of *A. mangium* plantation in SAFODA, Ulu Kukut, Sabah. Although *A. mangium* has important timber and non-timber applications, this devastating pathogen has forced many forest plantation companies to switch to other promising tree crops. This is the first investigation of the causal wilt pathogen in a commercial *A. mangium* plantation in Ulu Kukut, located in the western region of Sabah. Identifying the causal agent of wilt disease aid in developing effective disease management strategies in *Acacia*-based plantations and provide insight for ongoing and future projects on selecting suitable pruning treatments and identifying host responses to *C. manginecans* in *Acacia* species.

ACKNOWLEDGEMENTS

This research was supported by research grants Acculturation Grant Scheme (Code: SGA0080-2019) and UMSGreat (Code: GUG0466-1/2020) from Universiti Malaysia Sabah. The authors would like to express their sincere gratitude to Sabah Forest Development Authority (SAFODA), Ulu Kukut, for their invaluable assistance during the field sampling process. Special thanks are also extended to Dr. Marthin Tarigan from APRIL Fiber R&D for assisting with the transfer of *Ceratocystis* spores from carrot baiting and to Mr. Samsuddin Ahmad Syazwan from the Forest Research Institute Malaysia (FRIM) for assisting with the use of the MrBayes software.

REFERENCES

Al Adawi AO, Barnes I, Khan IA, Al Subhi AM, Al Jahwari AA, Deadman ML, Wingfield BD, Wingfield MJ. 2013. *Ceratocystis manginecans* associated with a serious wilt disease of two native legume trees in Oman and Pakistan. Australas Plant Pathol 42: 179-193. DOI: 10.1007/s13313-012-0196-5.

Al Adawi AO, Barnes I, Khan IA, Deadman ML, Wingfield BD, Wingfield MJ. 2014. Clonal structure of *Ceratocystis manginecans* populations from mango wilt disease in Oman and Pakistan. Australas Plant Pathol 43: 393-402. DOI: 10.1007/s13313-014-0280-0.

Al-Bedak OA, Mohamed RA, Seddek NH. 2018. First detection of *Neoscytalidium dimidiatum* associated with canker disease in Egyptian Ficus trees. For Pathol 48 (2): e12411. DOI: 10.1111/efp.12411.

Ambrose A, Liam J, Terhem R. 2022. New and emerging disease threats to forest plantations in Sarawak Borneo, Malaysia. Current and Emerging Challenges in the Diseases of Trees. IntechOpen. DOI: 10.5772/intechopen.107027.

Barnes I, Rauf MA, Fourie A, Japarudin Y, Wingfield M. 2023. *Ceratocystis manginecans* and not *C. fimbriata* a threat to propagated *Acacia* spp. in Sabah, Malaysia. J Trop For Sci 35: 16-26.

Bini D, dos Santos CA, Bouillet JP, Gonçalves JLM, Cardoso EJBN. 2013. *Eucalyptus grandis* and *Acacia mangium* in monoculture and intercropped plantations: Evolution of soil and litter microbial and chemical attributes during early stages of plant development. Appl Soil Ecol 63: 57-66. DOI: 10.1016/j.apsoil.2012.09.012.

Brawner J, Japarudin Y, Lapammu M, Rauf R, Boden D, Wingfield MJ. 2015. Evaluating the inheritance of *Ceratocystis acaciivora* symptom expression in a diverse *Acacia mangium* breeding population. Southern For: J For Sci 77 (1): 83-90. DOI: 10.2989/20702620.2015.1007412.

Chi NM, Thu PQ, Hinh TX, Dell B. 2019. Management of *Ceratocystis manginecans* in plantations of *Acacia* through optimal pruning and site selection. Australas Plant Pathol 48: 343-350. DOI: 10.1007/s13313-019-00635-1.

Chi NM. 2022. Pathogenicity of *Ceratocystis manginecans* in inoculated *Acacia* roots. Indian Phytopathol 75: 231-237. DOI: 10.1007/s42360-021-00418-z.

Coetzee MPA, Wingfield BD, Golani GD, Tjahjono B, Gafur A, Wingfield MJ. 2011. A single dominant *Ganoderma* species is responsible for root rot of *Acacia mangium* and *Eucalyptus* in Sumatra. Southern For: J For Sci 73 (3-4): 175-180. DOI: 10.2989/20702620.2011.639488.

EFSA Panel on Plant Health (PLH), Jeger M, Bragard C, Chatzivassiliou E, Dehnen-Schmutz K, Gilioli G, Miret JAJ, MacLeod A, Navarro MN, Niere B, Parnell S, Potting R, Rafoss T, Urek G, Bruggen AV, Van der Werf W, West J, Winter S, Santini A, Tsopelas P, Vloutoglou I, Pautasso M, Rossi V. 2016. Risk assessment and reduction options for *Ceratocystis platani* in the EU. EFSA J 14 (12): e04640. DOI: 10.2903/j.efsa.2016.4640.

Epron D, Nouvellon Y, Mareschal L, Moreira RM, Koutika L-S, Geneste B, Delgado-Rojas JS, Laclau JP, Sola G, Gonçalves JLM, Bouillet J-P. 2013. Partitioning of net primary production in *Eucalyptus* and *Acacia* stands and in mixed-species plantations: Two case-studies in contrasting tropical environments. For Ecol Manag 301: 102-111. DOI: 10.1016/j.foreco.2012.10.034.

Farid AM, Syazwan SA, Azrul WWM, Patahayah M, Salleh SM, Ong SP. 2018. Ceratocystis fimbriata: A white listed invasive alien species (IAS) causing wilt disease on *Acacia mangium* plantation. Forest Research Institute Malaysia.

Farid AM, Terhem R, Aswad RM, Agustini L, Ho WM, Indrayadi H, Hidayati N. 2023. Diseases of *Acacia* and control measures in the tropics. In Forest Microbiology (pp. 375-400). Academic Press. DOI: 10.1016/B978-0-443-18694-3.00012-2.

Friday JB, Keith L, Hughes F. 2015. Rapid ‘Ōhi ‘a Death (Ceratocystis Wilt of ‘Ōhi ‘a). Plant Dis 107: 1-3.

Fourie A, Wingfield MJ, Wingfield BD, Barnes I. 2015. Molecular markers delimit cryptic species in *Ceratocystis* sensu stricto. Mycol Prog 14: 1020. DOI: 10.1007/s11557-014-1020-0.

Fourie A, Wingfield MJ, Wingfield BD, Thu PQ, Barnes I. 2016. A possible centre of diversity in South East Asia for the tree pathogen, *Ceratocystis manginecans*. Infect Genet Evol 41: 73-83. DOI: 10.1016/j.meegid.2016.03.011.

Gill W, Eyles A, Glen M, Mohammed C. 2016. Structural host responses of *Acacia mangium* and *Eucalyptus pellita* to artificial infection with the root rot pathogen, *Ganoderma philippii*. Forest Pathol 46 (4): 369-375. DOI: 10.1111/efp.12286.

Glass NL, Donaldson GC. 1995. Development of primer sets designed for use with the PCR to amplify conserved genes from filamentous ascomycetes. Appl Environ Microbiol 61 (4): 1323-1330. DOI: 10.1128/aem.61.4.1323-1330.1995.

Glen M, Bougher NL, Francis AA, Nigg SQ, Lee SS, Irianto R, Barry KM, Beadle CL, Mohammed CL. 2009. *Ganoderma* and *Amauroderma* species associated with root-rot disease of *Acacia mangium* plantation trees in Indonesia and Malaysia. Australas Plant Pathol 38: 345-356. DOI: 10.1071/AP09008.

Hegde M, Palanisamy K, Yi JS. 2013. *Acacia mangium* Willd. - A fast-growing tree for tropical plantation. J For Environ Sci 29 (1): 1-14. DOI: 10.7747/jfs.2013.29.1.1.

IBM Corp. 2021. IBM SPSS Statistics for Windows, Version 28.0. IBM Corp, Armonk, NY.

Jacobs K, Bergdahl DR, Wingfield MJ, Halik S, Seifert KA, Bright DE, Wingfield BD. 2004. *Leptographium wingfieldii* introduced into North America and found associated with exotic *Tomicus piniperda* and native bark beetles. Mycol Res 108 (4): 411-418. DOI: 10.1017/S0953756204009748.

Jha SK. 2020. Identification and management of heart-rot fungi. Banko Janakari 30 (2): 71-77. DOI: 10.3126/banko.v30i2.33482.

Kashyap A, Planas-Marquès M, Capellades M, Valls M, Coll NS. 2021. Blocking intruders: Inducible physico-chemical barriers against plant vascular wilt pathogens. J Exp Bot 72 (2): 184-198. DOI: 10.1093/jxb/eraa444.

Koutika L-S, Richardson DM. 2019. *Acacia mangium* willd: Benefits and threats associated with its increasing use around the world. For Ecosyst 6: 1-13. DOI: 10.1186/s40663-019-0159-1.

Lapammu M, Warburton P, Japarudin Y, Boden D, Wingfield M, Brawner J. 2023. Verification of tolerance to infection by *Ceratocystis manginecans* in clones of *Acacia mangium*. J Trop For Sci 35: 42-50.

Lee KL, Ong KH, King PJH, Chubo JK, Su DSA. 2015. Stand productivity, carbon content, and soil nutrients in different stand ages of *Acacia mangium* in Sarawak, Malaysia. Turk J Agric For 39 (1): 154-161. DOI: 10.3906/tar-1404-20.

Lee SS. 2018. Observations on the successes and failures of *Acacia* plantations in Sabah and Sarawak and the way forward. J Trop For Sci 30: 468-475. DOI: 10.26525/jtfs2018.30.5.468475.

Lehtijärvi A, Oskay F, Doğmuş Lehtijärvi HT, Aday Kaya AG, Pecori F, Santini A, Woodward S. 2018 *Ceratocystis platani* is killing plane trees in Istanbul (Turkey). For Pathol 48 (1): e12375. DOI: 10.1111/efp.12375.

Lelana NE, Dendang B, Anggraeni I. 2020. Molecular identification of rust disease on *Acacia mangium* collected from West Java, Indonesia. IOP Conf Ser Earth Environ Sci 468: 012044. DOI: 10.1088/1755-1315/468/1/012044.

Li Y, Steenwyk JL, Chang Y, Wang Y, James TY, Stajich JE, Spatafora JW, Groenewald M, Dunn CW, Hittinger CT, Shen XX, Rokas A. 2021. A genome-scale phylogeny of the kingdom Fungi. Curr Biol 31 (8): 1653-1665. DOI: 10.1016/j.cub.2021.01.074.

Lopes UP, Zambolim L, Pinho DB, Barros AV, Costa H, Pereira OL. 2014. Postharvest rot and mummification of strawberry fruits caused by *Neofusicoccum parvum* and *N. kwambonambiense* in Brazil. Trop Plant Pathol 39 (2): 178-183. DOI: 10.1590/S1982-56762014000200009.

Maid M, Latif AA, Gan E, Salfinas N, Kitingan C, Maycock CR, Ratnam W. 2018. First report of stem canker disease on *Acacia mangium* induced by *Lasiodiplodia theobromae* and *Lasiodiplodia pseudotheobromae* species in Sabah, Malaysia. Malays Appl Biol 47 (3): 147-151.

Maid M, Ratnam W. 2014. Incidences and severity of vascular wilt in *Acacia mangium* plantations in Sabah, Malaysia. AIP Conf Proc 1614: 784-789. DOI: 10.1063/1.4895302.

Midgley SJ, Turnbull JW. 2003. Domestication and use of Australian acacias: Case studies of five important species. Aust Syst Bot 16 (1): 89-102. DOI: 10.1071/SB01038.

Mohammed CL, Barry KM, Irianto RSB. 2006. Heart rot and root rot in *Acacia mangium*: Identification and assessment. ACIAR Proc 124: 26-33.

Moller WJ, DeVay JE. 1968. Carrot as a species-selective isolation medium for *Ceratocystis fimbriata*. Phytopathology 58 (1): 123-124.

Nair PR, Kumar BM, Nair VD, Nair PR, Kumar BM, Nair VD. 2021. Multipurpose Trees (MPTs) and other agroforestry species. An Introduction to Agroforestry: Four Decades of Scientific Developments 281-351. DOI: 10.1007/978-3-030-75358-0_13.

Naranjo-Ortiz MA, Gabaldón T. 2019. Fungal evolution: Diversity, taxonomy and phylogeny of the Fungi. Biol Rev 94 (6): 2101-2137. DOI: 10.1111/brv.12550.

Newman L, Duffus ALJ, Lee C. 2016. Using the free program MEGA to build phylogenetic trees from molecular data. Am Biol Teacher 78 (7): 608-612. DOI: 10.1525/abt.2016.78.7.608.

Oliveira LSS, Guimarães LMS, Ferreira MA, Nunes AS, Pimenta LVA, Alfenas AC. 2015. Aggressiveness, cultural characteristics and genetic variation of *Ceratocystis fimbriata* on *Eucalyptus* spp. For Pathol 45 (6): 505-514. DOI: 10.1111/efp.12200.

Pornsuriya C, Sunpapao A. 2015. A new sudden decline disease of bullet wood in Thailand is associated with *Ceratocystis manginecans*. Australas Plant Dis Notes 10: 26. DOI: 10.1007/s13314-015-0176-z.

Raupp MJ, Gonthier P. 2017. Biotic factors: Pests and diseases. Routledge Handbook of Urban Forestry: 251-272. DOI: 10.4324/9781315627106-18.

Sitters J, Edwards PJ, Venterink HO. 2013. Increases of soil C, N, and P pools along an *Acacia* tree density gradient and their effects on trees

and grasses. Ecosystems 16: 347-357. DOI: 10.1007/s10021-012-9621-4.

Sudin M, Lee SS, Hj. Harun A. 1993. A survey of heart rot in some plantations of *Acacia mangium* in Sabah. J Trop For Sci 6 (1): 37-47.

Suryantini R, Wulandari RS. 2018. Diversity of Ganoderma pathogen in Pontianak, West Kalimantan: Characteristics, virulence and ability to infect *Acacia mangium* seedlings. Biodiversitas 19 (2): 465-471. DOI: 10.13057/biodiv/d190213.

Syazwan SA, Mohd-Farid A, Wan-Muhd-Azrul WA, Syahmi HM, Mohd Zaki A, Ong SP, Mohamed R. 2021. Survey, identification, and pathogenicity of *Ceratocystis fimbriata* complex associated with wilt disease on *Acacia mangium* in Malaysia. Forests 12 (12): 1782. DOI: 10.3390/f12121782.

Tamura K, Stecher G, Kumar S. 2021. MEGA11: Molecular evolutionary genetics analysis version 11. Mol Biol Evol 38 (7): 3022-3027. DOI: 10.1093/molbev/msab120.

Tarigan M, Roux J, Van Wyk M, Tjahjono B, Wingfield MJ. 2011a. A new wilt and dieback disease of *Acacia mangium* associated with *Ceratocystis manginecans* and *C. acaciivora* sp. nov. in Indonesia. S Afr J Bot 77 (2): 292-304. DOI: 10.1016/j.sajb.2010.08.006.

Tarigan M, Wingfield MJ, van Wyk M, Tjahjono B, Roux J. 2011b. Pruning quality affects infection of *Acacia mangium* and *A. crassicarpa* by *Ceratocystis acaciivora* and *Lasiodiplodia theobromae*. Southern For: J For Sci 73 (3-4): 187-191. DOI: 10.2989/20702620.2011.639498.

Thu PQ, Qynh DN, Dell B. 2012. *Ceratocystis* sp. causes crown wilt of *Acacia* spp. planted in some ecological zones of Vietnam. Proc Intl Conf Impact Climate Change For Pests Dis Trop 2012: 38-44.

Trang TT, Eyles A, Davies N, Glen M, Ratkowsky D, Mohammed C. 2018. Screening for host responses in *Acacia* to a canker and wilt pathogen, *Ceratocystis manginecans*. For Pathol 48 (1): e12390. DOI: 10.1111/efp.12390.

Udarbe MP, Hepburn AJ. 1986. Development of *Acacia mangium* as a plantation species in Sabah. In Australian Acacias in Developing Countries. Proceedings of an International Workshop held at The Forestry Training Centre, Gympie, Queensland, Australia. ACIAR Proc 16: 157-159.

Unchi S. 2010. A three-decade *Acacia mangium*. Sepilok Bull 12: 57-61.

Van Wyk M, Al Adawi AO, Khan IA, Deadman ML, Al Jahwari AA, Wingfield BD, Ploetz R, Wingfield MJ. 2007. *Ceratocystis manginecans* sp. nov., causal agent of a destructive mango wilt disease in Oman and Pakistan. Fungal Divers 27: 213-230.

Wingfield M, Wingfield B, Warburton P, Japarudin Y, Lapammu M, Rauf MA, Boden D, Barnes I. 2023. Ceratocystis wilt of *Acacia mangium* in Sabah: Understanding the disease and reducing its impact. J Trop For Sci 35: 51-66.

Wingfield MJ, Barnes I, de Beer ZW, Roux J, Wingfield BD, Taerum SJ. 2017. Novel associations between ophiostomatoid fungi, insects and tree hosts: Current status-future prospects. Biol Invasions 19: 3215-3228. DOI: 10.1007/s10530-017-1468-3.

Yadeta KA, Thomma BPHJ. 2013. The xylem as battleground for plant hosts and vascular wilt pathogens. Front Plant Sci 4: 97. DOI: 10.3389/fpls.2013.00097.